Biosensors and Bioelectronics 72 (2015) 87–94

Contents lists available at ScienceDirect

Biosensors and Bioelectronics

journal homepage: www.elsevier.com/locate/bios

Enhancing the speed of morpholino-DNA biosensor by electrokinetic concentration of DNA in a microfluidic chip

Diogo Martins [a], Rastislav Levicky [b], Yong-Ak Song [a,b,*]

[a] Division of Engineering, New York University Abu Dhabi, P.O. Box 129188, Abu Dhabi, UAE
[b] Department of Chemical and Biomolecular Engineering, New York University Polytechnic School of Engineering, Brooklyn, NY 11201, USA

ARTICLE INFO

Article history:
Received 18 February 2015
Received in revised form
13 April 2015
Accepted 20 April 2015
Available online 28 April 2015

Keywords:
Morpholino
DNA
Hybridization
Ion polarization concentration (ICP)
Microfluidics
Poly(3,4-ethylenedioxythiophene)-poly-styrene sulfonate (PEDOT:PSS)

ABSTRACT

Electrokinetic methods that conveniently concentrate charged analytes by orders of magnitude are highly attractive for nucleic acid assays where they can bypass the complexity and costs of enzyme-based amplification. The present study demonstrates an electrokinetic concentration device incorporating charge-neutral morpholino (MO) probes: as DNA analyte is concentrated in a microfluidic channel using ion concentration polarization (ICP) it is simultaneously hybridized to spots of complementary MO probes immobilized on the channel floor. This approach is uniquely favored by the match between the optimum buffer ionic strength of approximately 10 mM for both MO–DNA surface hybridization and electrokinetic concentration. The simple and easily scalable poly(dimethylsiloxane) (PDMS) microfluidic device was fabricated using soft lithography and contact printing of a conductive polymer, poly(3,4-ethylenedioxythiophene)-polystyrene sulfonate (PEDOT:PSS) as a cation-selective membrane material. Using the microfluidic concentrator, we could increase the concentration of DNA by three orders of magnitude in less than 5 min at an electric field of 75 V cm^{-1}. The 1000-fold increase in concentration of DNA led to an increase in the speed of MO–DNA hybridization by two orders of magnitude and enabled a detection sensitivity of ~1 nM within 15 min of concentration. Using the proposed microfluidic concentrator, we also demonstrated a rapid hybridization with a binary DNA mixture, containing a fully complementary and a non-complementary sequence to mimic molecular backgrounds present in real DNA samples.

1. Introduction

Perhaps the most important determinant of successful detection of an analyte is its concentration. In the case of nucleic acids, an effective, enzyme-free approach is to increase concentration through electrokinetic means (Kim et al., 2010). Although electrokinetic concentration works optimally at lower ionic strengths, such conditions suppress hybridization between the nucleic acid analyte and like charged DNA probes immobilized, for example, on a sensor surface (Fuchs et al., 2010; Gong and Levicky, 2008; Okahata et al., 1998). To overcome this shortcoming, the present study combines electrokinetic concentration of nucleic acid analyte with detection through hybridization to uncharged morpholino (MO) probes, which can readily hybridize with nucleic acids at favorably low ionic strengths. We envision this approach to ultimately provide a route toward concentration of DNA or RNA analyte without reliance on enzymatic amplification typically required by conventional assays.

MOs are synthetic nucleic acid analogs with a non-charged backbone of morpholine rings (Gong et al., 2010; Tercero et al., 2010, 2009). When substituted for DNA probes in surface hybridization applications, analyte detection becomes possible at low and moderate ionic strengths down to around 10 mM (Qiao et al., 2013), instead of the 0.1–1 M typically required with DNA probes (Gong and Levicky, 2008; Hassibi et al., 2009). Despite these advantages, MO-based assays nevertheless share the same limitations of conventional methods when it comes to analyte concentration, namely poor detection sensitivity and long hybridization durations at low concentrations (Janson and During, 2006; Wang and Smirnov, 2009). Poor detection sensitivity resulting from low target concentration is usually remedied by polymerase chain reaction (PCR) or other amplification prior to hybridization. However, amplification introduces sample processing that complicates assay workflow as well as can bias the sequence composition of the sample (Haddad et al., 2007; Ma et al., 2006; Pinard et al., 2006). Therefore, strong motivation exists for

* Corresponding author at: Division of Engineering, New York University Abu Dhabi, P.O. Box 129188, Abu Dhabi, UAE. Fax: +971 2 659 0794.
E-mail address: rafael.song@nyu.edu (Y.-A. Song).

http://dx.doi.org/10.1016/j.bios.2015.04.063
0956-5663/

developing alternate approaches for enhancing analyte concentration.

To enhance the MO–DNA hybridization assay speed and sensitivity, we propose integration of an ion concentration polarization (ICP)-based microfluidic concentrator with a MO microarray. The ICP concentrator collects target biomolecules from a ~μL sample volume and concentrates them into a ~nL plug in the vicinity of the capture probes (Kim et al., 2010; Ko et al., 2011; Wang and Han, 2008). ICP concentration not only reduces the analyte diffusion length but also increases the hybridization rate as a result of the locally enhanced concentration of biomolecules. Hence ICP-enhanced surface hybridization assays are expected to provide much faster detection than conventional assays without ICP enhancement.

Currently, several strategies are available to provide sample preconcentration in liquids, including isotachophoresis (Bercovici et al., 2012; Eid et al., 2013; Garcia-Schwarz and Santiago, 2012), field-amplified sample stacking (Bur and Chien, 1991), isoelectric focusing (O'Neill et al., 2006), electrokinetic trapping (Astorga-Wells and Swerdlow, 2003; Wang et al., 2005), micellar electrokinetic sweeping (Quirino and Terabe, 1998), chromatographic trapping (Yu et al., 2001), temperature-gradient focusing (Ross and Locascio, 2002), and membrane preconcentration (Rohr et al., 2001; Yu et al., 2001). Many of these techniques are originally developed for capillary electrophoresis, and require special buffer arrangements and/or reagents. Among these, we consider a coupling of the ICP-based electrokinetic concentration and the MO diagnostic platform as uniquely synergistic since both deliver optimal performance at moderate ionic strength (~10 mM) (Ko et al., 2012; Qiao et al., 2013). Additionally, ICP concentrators are straightforward in design and fabrication consisting of a single PDMS microchannel with an integrated Nafion ion-selective membrane (B. Kim et al., 2013a, M. Kim et al., 2013b; Ko et al., 2012). Based on this microfluidic concentrator concept, we have developed an ICP concentrator featuring, for the first time, a conductive polymer, poly(3,4-ethylenedioxythiophene)-poly(styrenesulfonate) (PEDOT:PSS) as a cation-selective membrane. To this end, PEDOT:PSS was printed on a glass substrate using a fluid microplotter (Cheun et al., 2006), instead of using the micro-flow patterning technique which is not reproducible (B. Kim et al., 2013a, M. Kim et al., 2013b), leads to variable membrane thicknesses (Lee et al., 2008), and allows for nanogaps along the membrane edge due to an incomplete PDMS bonding that may dominate the nanofluidic ICP phenomena (B. Kim et al., 2013a, M. Kim et al., 2013b). Microplotter dispensing of PEDOT:PSS is a flexible technique that allows for the deposition of discrete (spots), continuous (lines or arcs) or even three dimensional (multiple layers) features (Larson et al., 2004). PEDOT:PSS can also be processed using cleanroom fabrication techniques (Charlot et al., 2012). In particular, it can be deposited on a wafer substrate by spin coating and then patterned by UV lithography in conjunction with reactive ion etching. Such a fabrication capability of PEDOT:PSS polymer is highly advantageous since it allows building of a high-density array of concentrators on a large wafer scale.

In the present study, we built a single concentrator device by printing PEDOT:PSS next to a spotted array of capture MO oligomers and then reversibly sealing the slide using a PDMS microchannel. After characterizing the DNA concentration enhancement at different electric field strengths as a function of the concentration time, we compared the rates of MO/DNA surface hybridization without and with concentration. We also interrogated hybridization specificity using DNA target sequences having different numbers of nucleotide mismatches, from a fully non-complementary sequence down to a single-nucleotide mismatch. Lastly, we quantified the increase of hybridization speed in the presence of a fully non-complementary sequence added to a solution of fully complementary DNA under electrokinetic concentration. This study demonstrates potential applications of ICP-based microfluidic concentrators for improving the performance of solid phase DNA and RNA analysis.

2. Materials and methods

2.1. Materials

The unlabeled MO probe sequence PM1 and fluorescein isothiocyanate (FITC, λ_{exc}=494 nm and λ_{em}=518 nm) labeled PM2 in Table 1 were purchased from Gene Tools LLC. The FITC-labeled morpholino was used to verify the printing quality of MO probes on glass slides. The 20mer probes were modified with an amino group at the 5' end to allow for surface attachment to aldehyde groups on Superaldehyde 2 microarray slides from Arrayit. Cyanine 5 (Cy5, λ_{exc}=649 nm and λ_{em}=670 nm) and cyanine 3 (Cy3, λ_{exc}=550 nm and λ_{em}=570 nm) labeled DNA targets were purchased from Integrated DNA Technologies. For MO–DNA hybridization experiments, we used 25 nucleotides long oligonucleotides having different numbers (N) of nucleotide mismatches, as listed in Table 1: fully complementary target (N=0) TD1; single-nucleotide mismatch (N=1) strand TD2; 28% mismatch target (N=7) TD3; 48% mismatch target (N=12) TD4; and non-complementary target (N=25) TD5. These DNA targets were labeled at the 3'-end with Cy5 to enable fluorescence detection. Cy3-labeled non-complementary DNA target TD6 was combined with fully complementary TD1 in a 1:1 ratio to investigate ICP-enhanced surface hybridization in the presence of a non-complementary background. All hybridization solutions were prepared in 0.1 × PBS at pH 7.1 with no other additives. For storage, as received probes and targets listed in Table 1 were diluted with deionized (DI) water of 18 MΩ cm resistivity to a concentration of 200 μmol L^{-1} before storing at −20 °C. Conductive polymer PEDOT:PSS 2.2–2.6% in H_2O (high conductivity grade) was obtained from Sigma-Aldrich. Phosphate buffer saline (PBS) solution at 0.1 × pH 7.1 was prepared by diluting 10 × PBS purchased from Gibco. Sodium phosphate buffer (PB) of desired pH was prepared by combining monobasic sodium phosphate and dibasic sodium

Table 1
Morpholino probes and DNA target sequences.

Sequence	Abbreviation	Comments
5′ NH_2-GTA GCT AAT GAT GTG GCA TCG GTT 3′	PM1	MO probe
5′ NH_2-GTA GCT AAT GAT GTG GCA TCG GTT-FITC 3′	PM2	MO immobilization control
5′ CAA CCG ATG CCA CAT CAT TAG CTA C-Cy5 3′	TD1	Complementary DNA target
5′ CAA CCG ATG CCA **T**AT CAT TAG CTA C-Cy5 3′	TD2	2% mismatch (N=1) DNA target
5′ CAA C**AT** ATG C**TC** CA**G** CAT T**CT** CTA C-Cy5 3′	TD3	28% mismatch (N=7) DNA target
5′ **TC**A C**AT** AT**A** C**TC** CA**G** CAT T**CT** C**CC** C-Cy5 3′	TD4	48% mismatch (N=12) DNA target
5′ TGG AAT GCA TTG AGC AGC CGT AGC T-Cy5 3′	TD5	Non-complementary DNA target (N=25)
5′ TGG AAT GCA TTG AGC AGC CGT AGC T-Cy3 3′	TD6	Non-complementary DNA target Cy3 tagged

phosphate from Sigma-Aldrich in the appropriate proportions. Sodium borohydride ($NaBH_4$) and nonionic surfactant Tween 20 were purchased from Merck and Sigma-Aldrich, respectively. PDMS prepolymer set (Sylgard 184) was obtained from Dow Corning Inc.

2.2. Preparation of MO microarrays with integrated conductive polymer

To fabricate MO microarrays, 40 μmol L^{-1} PM1 in 0.1 M PB at pH 8.0 was printed using a fluid GIX microplotter II (Sonoplot Inc.) and a micro glass tip with a diameter of 50 μm (Sonoplot Inc.). After printing the PM1 spots, an additional array of fluorescent PM2 spots was printed for visual control of uniformity (Fig. S1 in Supplemental information). For surface hybridization in microchannels, we printed linear arrays of MO spots with ~50 μm diameters spaced by ~50 μm using the following dispensing settings: frequency 460 kHz, voltage 7.0 V, and time 0.5 s. After printing, slides were stored in a desiccator at 23 °C for 24 h.

Next, unbound MO probes were washed from the slide as follows. First, we concomitantly deactivated unreacted aldehyde groups to hydroxyl groups and reduced the labile Schiff base bonds between probes and the slide by washing slides in 100 mL of freshly prepared $NaBH_4$ solution (280 mg of $NaBH_4$, 24 mL of absolute ethanol, and 76 mL of PB 0.1 M pH 7.0) for 5 min (Qiao et al., 2013). The slides were then rinsed with DI water for 2 min. Next, a surfactant wash with 0.05% (w/v) Tween 20 solution for 5 min was used to remove physisorbed probes, followed by a second 2 min DI water rinse. Lastly, the slides were dried under a nitrogen stream.

After washing of the slides, a color dye was spotted on the slide corners as an alignment mark to allow an alignment between MO spots, PEDOT:PSS membrane, and the PDMS microchannel (Fig. S2 in Supplemental information). A circular PEDOT:PSS membrane with a diameter of 400–500 μm was then printed next to the array of the capture morpholino oligomers. A glass tip with an aperture of ~200 μm was used for contact printing of a circular PEDOT:PSS layer on the aldehyde slide surface. The thickness of the conductive polymer layer was dependent on the surface contact duration, where a contact period of 30 s resulted in a ~3 μm thick membrane (see Fig. S3 in Supplemental information). For a reproducible ICP-based concentration, it was required to stir the PEDOT:PSS solution vigorously before printing. After contact printing of PEDOT:PSS layers, slides were dried at room temperature for 30 min.

2.3. Experimental setup

For all ICP concentration experiments, the PDMS microchannel was first treated with air plasma (Plasma cleaner, from Harrick Plasma) for 1 min before assembling it onto the glass slide (Fig. S4 in Supplemental information) to enable spontaneous filling with DNA sample solutions. 100 μL of 0.1 × PBS buffer was first loaded into one of the reservoirs, thus filling the microchannel up to the edge of the opposite reservoir by capillarity. After equilibrating the conductive polymer membrane for 20 min, 50 μL of DNA target solution was loaded into the opposite reservoir and a voltage was applied along the microchannel through Pt wire electrodes using a DC source meter (Keithley 2400). For diffusion-limited MO–DNA hybridization experiments without electrokinetic concentration, the microchannel was simply filled with a DNA target solution by loading the reservoirs with 100 μL of the same solution and then incubated at room temperature. An adhesive tape was used to seal each reservoir and to prevent evaporation.

All the experiments were imaged using an inverted epi-fluorescence microscope (Nikon Ti-Eclipse) equipped with a mercury lamp (Nikon Intensilight C-HGFIE), a digital camera (Andor Clara), and an electronic shutter (Lambda SC, from Sutter Instrument) to minimize photobleaching. Cy5 filter was used to observe fluorescence emission (λ_{em}=670 nm) of the DNA sample. The exposure time used for capture of the fluorescence signal was 2 s. For time-lapse imaging, the shutter was synchronized with the camera exposure and images were captured at 5 s intervals. To prevent saturation of the CCD camera during time-lapse acquisitions a set of neutral-density filters was used as needed.

2.4. Data analysis

Fluorescent images were analyzed using NIH ImageJ. To quantify the DNA concentration in the plug, we measured the fluorescence intensity of the microchannel filled with DNA samples of known concentrations (0.1, 1, 10, and 100 μM) and used them as references. To estimate the plug length, we isolated the plug pixels in the images by thresholding the images using ImageJ and setting the fluorescence intensity of the initial DNA solution as the threshold limit. Hybridization intensity of a MO–DNA spot was determined by measuring the average intensity of the pixels belonging to the spot and then subtracting the background signal given by the average intensity of the pixels around that same spot. For hybridization experiments without ICP concentration, intensities measured from 5 to 6 spots were combined to provide final averaged values and standard deviations. In experiments with ICP concentration, only those MO–DNA spots with uniform fluorescence signal intensity that were located directly under the concentration plug were selected for quantitative analysis.

3. Results and discussion

3.1. Device design and operation

A schematic of the microfluidic concentrator is presented in Fig. 1. It consists of a PEDOT:PSS layer, printed directly on the bottom of a microchannel next to an array of MO capture probes, and a reversibly sealed PDMS microchannel from the top with two reservoirs and electrodes. 100 μL of 0.1 × PBS was dispensed into the cathodic reservoir and 50 μL of DNA sample was dispensed into the anodic reservoir. This volume difference generated a pressure-driven flow of the buffer solution into the DNA sample reservoir, which prevented the DNA molecules from diffusing out of the reservoir prior to the start of a concentration experiment and also washed off the MO–DNA hybridization spot at the end of surface hybridization once the voltage was switched off. The voltage difference generated an electroosmotic flow (EOF) in the opposite direction to the pressure-driven flow and transported the biomolecules towards the conductive polymer layer. Because PEDOT:PSS is negatively charged, it acts as a cation-selective membrane that conducts cations away and thus generates an ion depletion region in front of the conductive polymer layer, which in combination with the EOF carrying the sample molecules leads to formation of a plug with enhanced DNA concentration. Bipolar electrode focusing (Anand et al., 2011a,b; Knust et al., 2012; Song et al., 2014) provides an alternative potential explanation for the preconcentration mechanism. The simplicity of this concentrator makes this concentration scheme highly scalable. In fact, by combining micro contact printing of suitably patterned PEDOT:PSS membranes and reversible sealing with a PDMS microchannel, it should be possible to integrate our concentrator onto existing microarrays to enable hybridization assays in a highly multiplexed manner.

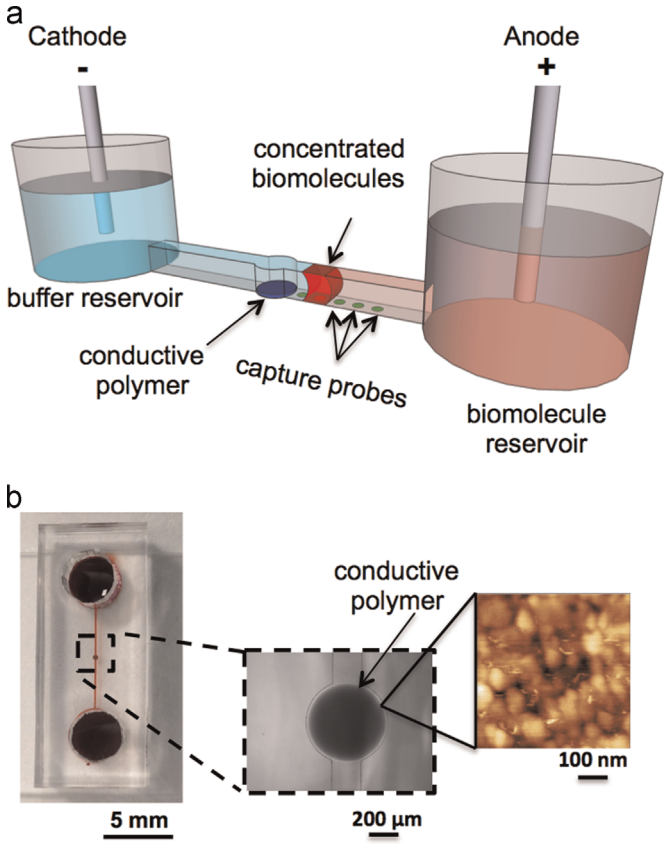

Fig. 1. A microfluidic ICP concentrator for enhancing the detection sensitivity and speed of MO–DNA biosensing. (a) 3-D schematic of the concentrator with a DNA concentration plug incubated over surface-printed spots of MO probes. (b) Photograph of a microfluidic concentrator showing a single microchannel (17 μm high; 1 cm long; 200 μm wide) in PDMS with a reservoir (4 mm of diameter) at each end. An ion-selective PEDOT:PSS circular layer (~3.0 μm high; 400–500 μm in diameter) is printed on the bottom center of the microchannel. The AFM image shows the surface structure of the PEDOT:PSS layer.

3.2. Characterization of electrokinetic DNA concentration

To characterize the concentration performance of our device, DNA sample (TD1) with an initial concentration of 10 nM was concentrated using three different voltages (30, 50, and 75 V) applied between the Pt electrodes. Above 75 V, a rapid degradation of the conductive polymer layer was observed within a few minutes and therefore such high voltages were not usable for electrokinetic concentration. When a DC voltage between 30 and 75 V was applied at both reservoirs, a fluorescent plug started forming in front of the conductive polymer (see compressed-time Video1 in Supplemental material). After 5 min of concentration, a bright fluorescent plug was visible inside the channel indicating concentrated DNA near the conductive polymer membrane and its size continued to increase as a function of the concentration time, as shown in Fig. 2a. With increasing voltage, stronger vortices were observed in the depletion region. As the fluorescence signal intensity graph in Fig. 2b shows, DNA concentration increased rapidly from $C_0=10$ nM to $C>1$ μM in less than a minute and then stabilized after about 5 min. Higher voltages resulted in higher DNA concentrations; however, the DNA plug was less stable due to the strong vortex formation in the depletion zone. With this approach, a concentration factor of ~1000 was obtained at 75 V in less than 5 min and was maintained near the conductive polymer layer for ~25 min, while for 50 V and 25 V the DNA plug remained near the membrane for ~32 min and ~44 min, respectively. The electrical currents measured at these voltages were as follows:

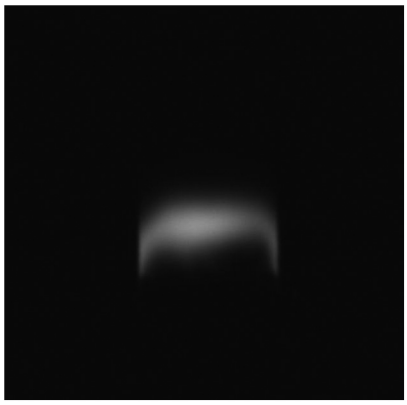

Video 1. Compressed-time video (approximately 33 min. real time) of DNA concentration in the microfluidic concentrator starting from an initial DNA concentration of 10 nM in 0.1X pH 7.1 PBS buffer at 50 V across the microchannel.. A video clip is available online. Supplementary material related to this article can be found online at http://dx.doi.org/10.1016/j.bios.2015.04.063.

1.3 μA for 30 V, 2.4 μA for 50 V, and 3.8 μA for 75 V. When concentrated beyond these times, the sample plug burst in the direction of the sample reservoir. The length of the plug increased roughly at a constant rate of ~5 μm min^{-1}, between 50 and 135 μm, as shown in Fig. 2c. The applied voltage did not show any significant influence on the length of the plug, up to $t=20$ min.

3.3. Surface hybridization of a single DNA target under electrokinetic concentration

Application of 75 V along a microchannel in the presence of immobilized MO probes resulted in ICP concentration zones similar to those obtained with unspotted slides (see Video2 provided as Supplemental material). This is seen in Fig. 3a, where again the DNA concentration was locally increased by ~three orders of magnitude within 15 min, showing that the presence of electrically neutral MO probes on the slide does not affect the electrokinetic sample concentration. This feature is a significant advantage for integration of electrokinetic concentrators with MO microarrays. In addition, ICP-enhanced the rate of hybridization significantly compared to standard methods. After concentrating the target DNA on the MO spots for only 15 min, we could achieve a comparable fluorescent signal intensity to that realized without ICP after 150 min at $C_0=100$ nM, 210 min at $C_0=10$ nM, and 16 h at $C_0=1$ nM, as shown in Fig. 3a. The limit of detection (LOD) for the ICP-enhanced hybridization was 1 nM after 15 min. If hybridization rate is assessed from the time required by both hybridization methods to reach the same signal, within 15 min we could achieve an increase in the rate of 10-fold for $C_0=100$ nM, 14-fold for $C_0=10$ nM, and about 64-fold for $C_0=1$ nM by utilizing the concentrator. The higher fold improvements as target concentration decreased are attributed to greater benefit of ICP concentration under such mass transfer limited conditions. In general, the rate of hybridization reflects both mass transport and reaction kinetic limitations; however, given a lack of information on the ICP flow pattern and the three dimensional DNA concentration profile no attempt was made to separate mass transport from kinetic contributions. Experiments targeted at clarifying the ICP flow pattern and how it affects delivery of analyte to the solid support will be undertaken in the future.

Fig. 3b shows the fluorescence images of the MO probes after hybridization, without and with ICP. Non-specific adsorption of DNA fragments to the substrate was negligible, even when DNA was concentrated by ICP. Therefore, no additional surface passivation step was required such as surface coating with BSA or PLL-

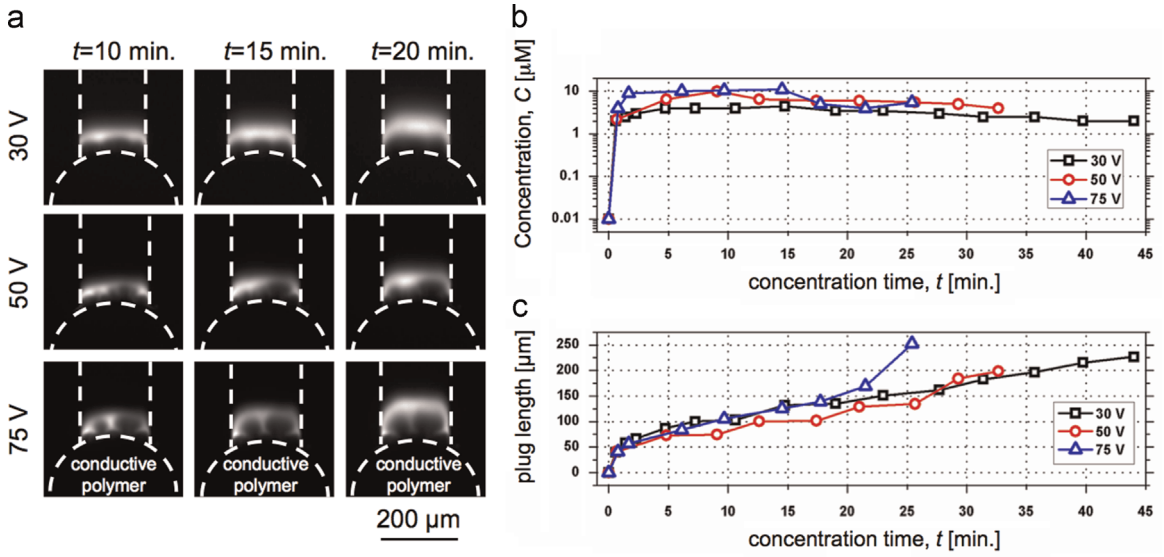

Fig. 2. Characterization of DNA concentration in the microfluidic concentrator at an initial DNA concentration of 10 nM in 0.1 × pH 7.1 PBS buffer at different voltages. (a) Formation of a DNA concentration plug at different applied voltages and concentration times. At all three voltage settings, the DNA plug remained close to the conductive polymer. Strong vortex formation could be observed in the depletion zone at 75 V. (b) The DNA concentration increased rapidly in the first minute (from $C=10$ nM to more than $C>1$ μM) and then stabilized after about 5 min. Higher applied voltages generated somewhat higher DNA concentrations; however, the plug was less stable due to vortex formation. The maximum stable concentration time was ~25 min, ~32 min and ~44 min for 75 V, 50 V, and 25 V, respectively. (c) Length of the concentration plug as a function of time and for different voltages (30 V; 50 V; 75 V). The length of the plug and the rate of increase in size were almost independent of the applied voltage up to $t=20$ min.

PEG for these experiments.

3.4. Surface hybridization of complementary and non-complementary mixtures under electrokinetic concentration

Typical DNA samples contain other sequences that act as molecular backgrounds to the target sequence. To partially mimic the molecular backgrounds present in real samples, we added a non-complementary DNA TD6 to the complementary one, TD1, and repeated the hybridization experiment. As a reference, we performed hybridization experiments for a single complementary DNA (TD1) and a binary DNA sample containing equimolar amounts of TD1 complementary target and TD6 non-complementary DNA in overnight (12–15 h) incubations. The DNA sequences in the binary DNA mixture solution were tagged with two different fluorophores (TD1 and TD6 were Cy5 and Cy3 tagged, respectively) to investigate if the electrokinetic concentration of complementary DNA target TD1 was affected by a simultaneous concentration of TD6. As shown in Fig. 4a, the Cy5 fluorescence intensities of the plugs for the single and the binary mixture both increased by ~1000-fold, showing that the presence of TD6 in solution did not significantly impact the electrokinetic

Video 2. Compressed-time video of enhanced MO-DNA surface hybridization with ICP concentration starting from an initial DNA concentration of 10 nM in 0.1X pH 7.1 PBS buffer for 15 min. at 75 V across the microchannel. Supplementary material related to this article can be found online at http://dx.doi.org/10.1016/j.bios.2015.04.063.

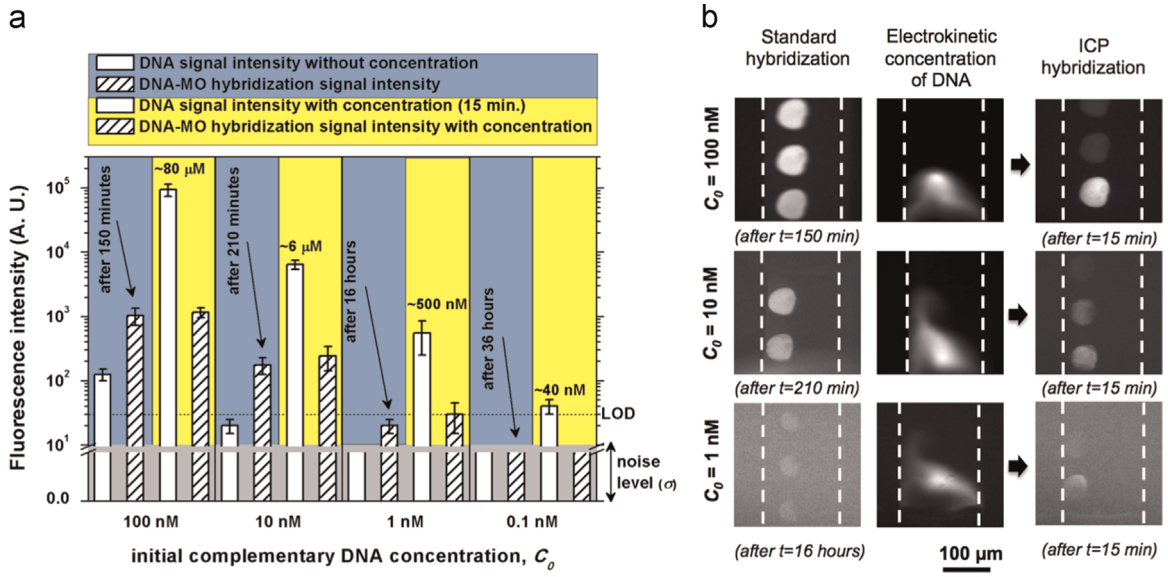

Fig. 3. Comparison of MO–DNA surface hybridization with and without ICP concentration. (a) Hybridization times needed to realize the same fluorescence intensity without and with 15 min ICP concentration, for different initial target concentrations C_0 ranging from 0.1 nM to 100 nM. ICP enabled faster hybridization by 10-fold for $C_0=100$ nM, 14-fold for $C_0=10$ nM and 64-fold for $C_0=1$ nM. Signals for $C_0=0.1$ nM were below noise level σ of the fluorescence background, $\sigma=10$ AU. The LOD (LOD$=3\times\sigma$) was set to 30 AU. At least three independent measurements were taken under the same test condition to ensure reproducibility and statistical significance of the experiments. (b) Fluorescence micrographs of (left) hybridized slides without ICP, (middle) ICP-concentrated DNA plugs in the presence of a linear array of MO spots on the bottom of the microchannel, and (right) hybridized slides after ICP-enhanced hybridization for 15 min at $C_0=1$, 10, and 100 nM.

concentration of TD1.

However, it is evident that presence of the non-complementary DNA TD6 did perturb surface hybridization of the complementary DNA TD1, as suggested by more than half an order of magnitude decrease of TD1 signal between the pure complementary and the binary mixture, observed at both $C_0=10$ nM and $C_0=100$ nM. In the case of the 10 nM DNA mixture, the hybridization signal intensity under electrokinetic concentration after 15 min was only about ~40% of the signal for an electrokinetically-concentrated solution of just the complementary target. For the 100 nM mixture, the signal intensity was ~50% of that for just the complementary target with ICP concentration. A similar trend, in which the hybridization signal for the mixture decreased relative to that for the pure TD1 target, was observed without ICP concentration. A possible explanation for these observations involves binding between TD1 and TD6 in solution. Since the six bases at the 3'-end of the TD1 and TD6 sequences (Table 1) are complementary, they could hybridize in solution what would present

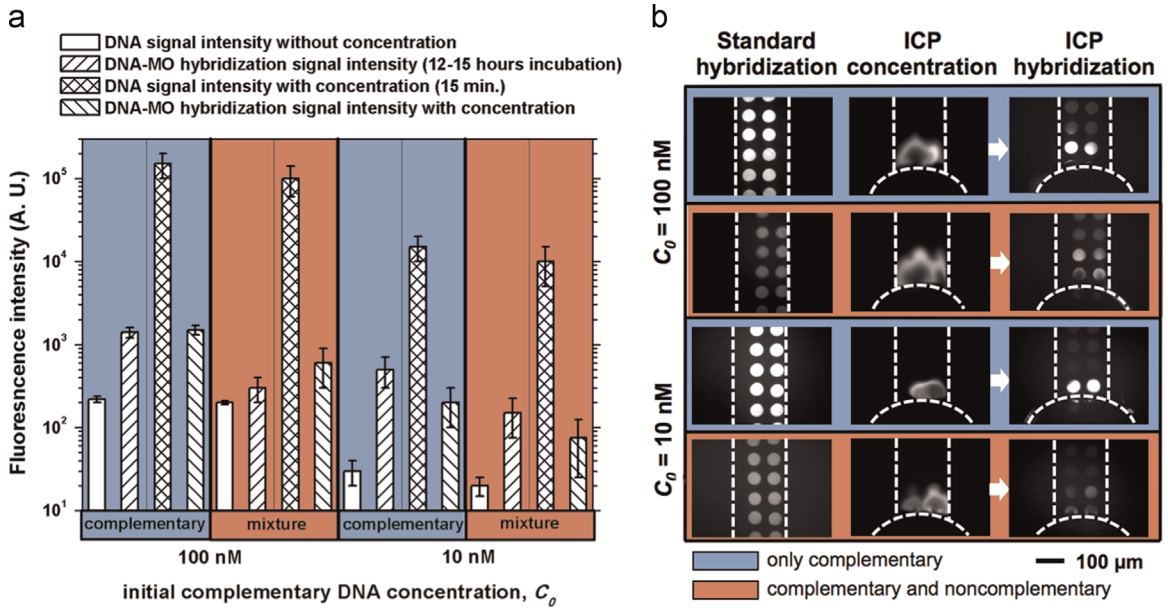

Fig. 4. (a) Comparison of fluorescence signal intensities with and without ICP enhancement for solutions containing just the fully complementary TD1 target as well as mixtures with equimolar concentration of fully complementary (TD1) and non-complementary (TD6) targets, at $C_0=10$ nM and 100 nM. Although hybridization of the mixture showed a loss in fluorescence signal intensity compared to that of the purely complementary solution, "with ICP" data suggests that DNA detection (down to the nanomolar range) in the presence of a complex media is possible within just 15 min. Data shown are the average of at least three experiments under the same test conditions with range bars representing the standard deviation. (b) Fluorescence micrographs showing the difference between without ICP and with ICP hybridization. Left column: hybridization without ICP; middle column: images of concentrated plugs after 15 min of ICP; right column: hybridization with ICP. The brightness and contrast of the images have been adjusted for optimal visualization, but for each DNA concentration of 10 nM or 100 nM the same brightness and contrast settings were applied for visual comparison.

both a kinetic activation barrier as well as a thermodynamic penalty to surface hybridization. Although UNAFOLD (Markham and Zuker, 2008) based estimates of the melting temperature indicate a range between −10 °C and 16 °C depending on strand concentration (i.e. solution or concentrated plug), so that most strands should be separated, the actual melting transitions could be significantly higher due to stabilization by the Cy5 and Cy3 labels (Fegan et al., 2008) as well as the unknown elevation in ionic strength within the ICP region. Despite the loss in fluorescence intensity, hybridization signals increased above the LOD and became detectable after only 15 min of electrokinetic concentration. This result delivered the first proof of concept that our concentration strategy for enhancing detection speed also works in DNA mixtures with molecular backgrounds.

3.5. *Sequence specificity of MO–DNA surface hybridization under electrokinetic concentration*

The sequence specificity of MO–DNA surface hybridization under ICP conditions was investigated with 100 nM DNA solutions, each solution containing a target sequence with a different percentage of mismatches from 0% to 100% (sequences TD1–TD5 in Table 1). As illustrated in Fig. 5, the ICP-enhanced hybridization assay could distinguish between 28% complementary ($N=7$) or higher (i.e. $7 < N \leq 25$) and the fully complementary DNA ($N=0$), but not between a single base mismatch ($N=1$) and the fully complementary DNA ($N=0$). The same sequence specificity was also obtained in MO–DNA surface hybridizations without ICP concentration (Fig. S5 in Supplemental information). This result indicates that application of an ICP concentration step does not influence the specificity of MO–DNA interactions. The presence of a fluorescence signal for $N=0$ and $N=1$ sequences and the absence of a fluorescence signal in the cases of $7 \leq N \leq 25$ sequences clearly indicates that the measured signal originates from targets that hybridized with the immobilized MO probes and not from the emission based non-specific adsorption. The lack of selectivity at the single mismatch level could potentially be addressed by adjusting the stringency of hybridization, as for conventional hybridization assays, through adjustments in temperature, ionic strength, or denaturant concentration (Benters et al., 2002; Guo et al., 1994). Another possible approach to achieve single base mismatch detection could be the integration of a highly sensitive, selective and label-free MO-functionalized silicon nanowire platform to the concentrator (Zhang et al., 2010).

4. Conclusions

Surface hybridization reactions are indispensable to genomic research. In microarray technologies, these reactions allow thousands of DNA or RNA sequences to be analyzed in a single experiment. Due to limited sample quantities, however, researchers have to usually employ PCR or other amplification of collected specimens to generate sufficient material to drive the hybridization reaction forward. The proposed concentrator with integrated conductive polymer in a microfluidic chip format provides a possible alternative to enzymatic amplification, in that the DNA or RNA sample concentration is increased electrokinetically directly at the location of capture probes. The higher concentrations allow faster detection of lower-abundancy sequences. Electrokinetic concentration also avoids artifacts that can arise during enzyme-based manipulation (e.g. amplification) of nucleic acid samples (Brakenhoff et al., 1991; Keohavong and Thilly, 1989; Thompson et al., 2002). Our biomolecular concentrator-based approach could be especially advantageous in settings where materials or facilities are not available for PCR or other amplification, such as in resource-poor settings without trained personnel and equipment.

As proof of concept, we integrated an ICP microfluidic concentrator to a morpholino microarray to increase the speed of hybridization of DNA targets to covalently immobilized MO probes. By enhancing the DNA target concentration by three orders of magnitude we could accelerate the MO–DNA reaction rate by up to 64-fold relative to hybridization without ICP enhancement; this corresponds to an effective reduction in incubation time from 16 h to 15 min, for a diluted DNA solution of 1 nM. Hybridization acceleration was also observed in the presence of a 1:1 background of a non-complementary DNA sequence in solution. To further increase detection sensitivity, different approaches can be considered including further reducing the diffusion distance of target analytes through use of permselective membranes with higher concentration capability and/or microchannels with smaller dimensions (e.g. ~5 μm height). With regard to sequence selectivity, specificity down to single mismatches should be possible through incorporation of more stringent hybridization conditions.

In the future, this class of concentrator-enhanced biosensors

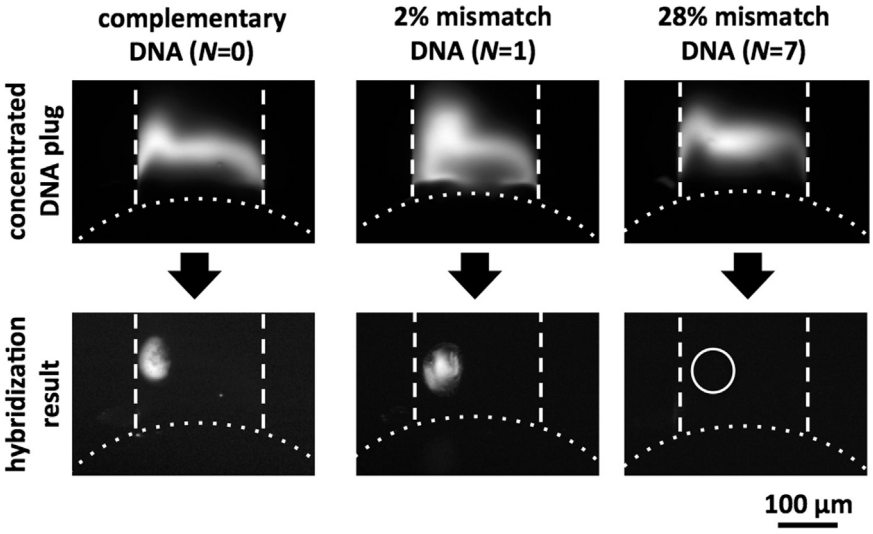

Fig. 5. Fluorescence images of sequence specificity assays under electrokinetic concentration using DNA targets with different numbers N of mismatched bases. From the left: $N=0$, $N=1$, and $N=7$ at an initial concentration of $C_0=100$ nM. The upper fluorescence images show the DNA plugs after 15 min of concentration at an electric field of 75 V cm^{-1}, and the lower fluorescence images show the corresponding hybridization results.

may become an indispensable high-throughput tool for "omics" technologies. We believe that our proposed concentrator is highly scalable and can be easily adapted to a high-density format, and used to conduct rapid large-scale quantitative experiments. In addition to nucleic acid analysis, our electrokinetic concentrator platform can be easily extended to other types of assays involving charged analytes, including immunoassays and other protein-based analyses.

Acknowledgments

We gratefully acknowledge the financial support from the New York University Abu Dhabi (NYUAD) through the NYUAD Research Enhancement Fund (RE092) 2013. The device fabrication was conducted in the microfabrication core facility of NYUAD.

Appendix A. Supplementary material

Supplementary data associated with this article can be found in the online version at http://dx.doi.org/10.1016/j.bios.2015.04.063.

References

Anand, R.K., Sheridan, E., Hlushkou, D., Tallarek, U., Crooks, R.M., 2011a. Lab Chip 11, 518–527.
Anand, R.K., Sheridan, E., Knust, K.N., Crooks, R.M., 2011b. Anal. Chem. 83, 2351–2358.
Astorga-Wells, J., Swerdlow, H., 2003. Anal. Chem. 75, 5207–5212.
Benters, R., Niemeyer, C.M., Drutschmann, D., Blohm, D., Wöhrle, D., Gmbh, C.B., Heerstrasse, S., Molekulare, B., 2002. Nucleic Acids Res. 30, e10.
Bercovici, M., Han, C.M., Liao, J.C., Santiago, J.G., 2012. Proc. Natl. Acad. Sci. USA 109, 11127–11132.
Brakenhoff, R.H., Schoenmakers, J.G.G., Lubsen, N.H., 1991. Nucleic Acids Res. 19 1949–1949.
Bur, D.S., Chien, R., 1991. Anal. Chem. 63, 2042–2047.
Charlot, B., Sassine, G., Garraud, A., Sorli, B., Giani, A., Combette, P., 2012. Microsyst. Technol. 19, 895–903.
Cheun, H., Rugheimer, P.P., Larson, B.J., Gopalan, P., Lagally, M.G., Winokur, M.J., 2006. J. Appl. Phys. 100, 073510.
Eid, C., Garcia-Schwarz, G., Santiago, J.G., 2013. Analyst 138, 3117–3120.
Fegan, A., Shirude, P.S., Balasubramanian, S., 2008. Chem. Commun. 2, 2004–2006.
Fuchs, J., Fiche, J.-B., Buhot, a, Calemczuk, R., Livache, T., 2010. Biophys. J. 99, 1886–1895.
Garcia-Schwarz, G., Santiago, J.G., 2012. Anal. Chem. 84, 6366–6369.
Gong, P., Levicky, R., 2008. Proc. Natl. Acad. Sci. USA 105, 5301–5306.
Gong, P., Wang, K., Liu, Y., 2010. J. Am. Chem. Soc. 132, 9663–9671.
Guo, Z., Guilfoyle, R. a, Thiel, A.J., Wang, R., Smith, L.M., 1994. Nucleic Acids Res. 22, 5456–5465.
Haddad, F., Qin, A.X., Giger, J.M., Guo, H., Baldwin, K.M., 2007. BMC Biotechnol. 7, 14.
Hassibi, A., Vikalo, H., Riechmann, J.L., Hassibi, B., 2009. Nucleic Acids Res. 37, e132.
Janson, C.G., During, M.J., 2006. Peptide Nucleic Acids, Morpholinos and Related Antisense Biomolecules. Landes Bioscience/Eurekah.com and Kluwer Academic/Plenum Publishers, New York.
Keohavong, P., Thilly, W.G., 1989. Proc. Natl. Acad. Sci. USA 86, 9253–9257.
Kim, B., Heo, J., Kwon, H.J., Cho, S.J., Han, J., Kim, S.J., Lim, G., 2013. ACS Nano 7, 740–747.
Kim, M., Jia, M., Kim, T., 2013. Analyst 138, 1370–1378.
Kim, S.J., Song, Y.-A., Han, J., 2010. Chem. Soc. Rev. 39, 912–922.
Knust, K.N., Sheridan, E., Anand, R.K., Crooks, R.M., 2012. Lab Chip 12, 4107–4114.
Ko, S.H., Kim, S.J., Cheow, L.F., Li, L.D., Kang, K.H., Han, J., 2011. Lab Chip 11, 1351–1358.
Ko, S.H., Song, Y.-A., Kim, S.J., Kim, M., Han, J., Kang, K.H., 2012. Lab Chip 12, 4472–4482.
Larson, B.J., Gillmor, S.D., Lagally, M.G., 2004. Rev. Sci. Instrum. 75, 832.
Lee, J.H., Song, Y.-A., Han, J., 2008. Lab Chip 8, 596–601.
Ma, C., Lyons-Weiler, M., Liang, W., LaFramboise, W., Gilbertson, J.R., Becich, M.J., Monzon, F. a, 2006. J. Mol. Diagn. 8, 183–192.
Markham, N.R., Zuker, M., 2008. Bioinformatics, Volume II. Structure, Functions and Applications. Humana Press, New Jersey.
O'Neill, R. a, Bhamidipati, A., Bi, X., Deb-Basu, D., Cahill, L., Ferrante, J., Gentalen, E., Glazer, M., Gossett, J., Hacker, K., Kirby, C., Knittle, J., Loder, R., Mastroieni, C., Maclaren, M., Mills, T., Nguyen, U., Parker, N., Rice, A., Roach, D., Suich, D., Voehringer, D., Voss, K., Yang, J., Yang, T., Vander Horn, P.B., 2006. Proc. Natl. Acad. Sci. USA 103, 16153–16158.
Okahata, Y., Kawase, M., Niikura, K., Ohtake, F., Furusawa, H., Ebara, Y., 1998. Anal. Chem. 70, 1288–1296.
Pinard, R., de Winter, A., Sarkis, G.J., Gerstein, M.B., Tartaro, K.R., Plant, R.N., Egholm, M., Rothberg, J.M., Leamon, J.H., 2006. BMC Genomics 7, 21.
Qiao, W., Kalachikov, S., Liu, Y., Levicky, R., 2013. Anal. Biochem. 434, 207–214.
Quirino, J.P., Terabe, S., 1998. Science 282 (5388), 465–468.
Rohr, T., Davey, M.H., Fréchet, J.M.J., Berkeley, E.O.L., 2001. Electrophoresis 22, 3959–3967.
Ross, D., Locascio, L.E., 2002. Anal. Chem. 74, 2556–2564.
Song, H., Wang, Y., Garson, C., Pant, K., 2014. Anal. Methods 00, 1–7.
Tercero, N., Wang, K., Gong, P., Levicky, R., 2009. J. Am. Chem. Soc. 131, 4953–4961.
Tercero, N., Wang, K., Levicky, R., 2010. Langmuir 26, 14351–14358.
Thompson, J.R., Marcelino, L.A., Polz, M.F., 2002. Nucleic Acids Res. 30, 2083–2088.
Wang, X., Smirnov, S., 2009. ACS Nano 3, 1004–1010.
Wang, Y.-C., Han, J., 2008. Lab Chip 8, 392–394.
Wang, Y.-C., Stevens, A.L., Han, J., 2005. Anal. Chem. 77, 4293–4299.
Yu, C., Davey, M.H., Svec, F., Fre, J.M.J., Berkeley, E.O.L., 2001. Anal. Biochem. 73, 5088–5096.
Zhang, G.-J., Luo, Z.H.H., Huang, M.J., Tay, G.K.I., Lim, E.-J.A., 2010. Biosens. Bioelectron. 25, 2447–2453.